# Proximity Sensing for Robotics

R. E. Saad
*University of Toronto*

A. Bonen
*University of Toronto*

K. C. Smith
*University of Toronto*

B. Benhabib
*University of Toronto*

The objective of this chapter is to review the state-of-the-art in proximity-sensing technologies for robotics. Special attention is paid to the sensing needs of robotic manipulators for grasping applications, in contrast to the needs of mobile robots for navigation purposes. For a review of the application of proximity sensing to mobile robots, the reader is referred to [1].

Robotic sensors can be categorized into three groups: medium-range (object recognition and gross position/orientation estimation) sensors, short-range (proximity) sensors, and contact sensors. Recent literature [2–6] suggests that robotic end effectors should be equipped with both short-range proximity and contact sensors.

Proximity sensors should be able to measure the position and orientation (pose) of an object's surface. The range must be sufficiently large to compensate for uncertainties in the medium-range pose-estimation process, while maintaining sufficient accuracy to permit effective grasping of the object.

Transducers used by current proximity sensors vary in sophistication. Despite their great variety, however, these transducers and their accompanying electronic interface circuits (together comprising the proximity sensor) cannot presently meet the stringent robustness requirements of most industrial robotic applications. Novel sensing algorithms and techniques still must be developed in order to improve on their current characteristics, and, furthermore, to control both the sensing and grasping processes.

## 8.1  Proximity Definition

The term "proximity," quantified by "pose" in this chapter, refers to three geometrical parameters $x$, $u$, and $v$ as shown in Figure 8.1, where:

  $x$ = the translation from the origin of the sensor's reference coordinate frame, $F_p$, to a target point on the surface of the object measured along $X_p$. This target point defines the origin of the surface-frame, $F_r$

  $u$ = the *vertical* orientation of the object's surface, defined as a rotation around $Y_p$ (of the translated frame), thereby specifying the new $Z_r$

  $v$ = the *horizontal* orientation of the object's surface, defined as a rotation around $Z_r$, thereby specifying $Y_r$.
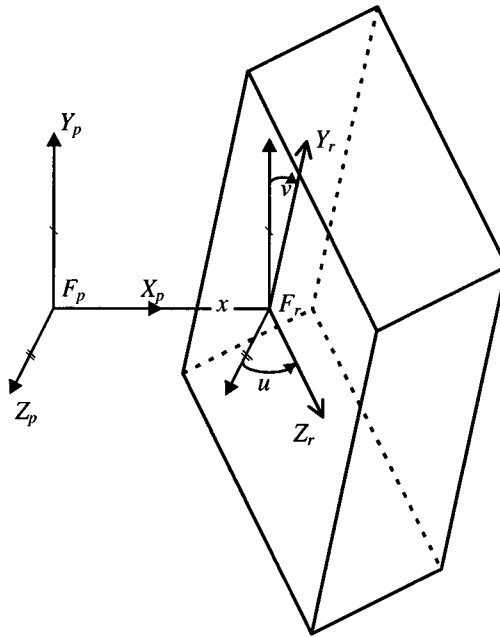
**FIGURE 8.1**  Proximity parameters.

## 8.2   Typical Sensor Characteristics

Conventionally, proximity sensors should be capable of measuring distances of up to 50 mm, and two degree-of-freedom orientations equivalent to an overall inclination of up to ±30°. The intended principal application of the sensor is to act as a guide for the robot. Thus, it would be desirable to have higher sensitivity and accuracy as the gripper approaches the object, namely when both the relative orientation and the distance approach near-zero values.

The signals received by the electronic interface circuit should be processed without limiting the required operating range of the sensor. The interface circuit should also minimize the effect of interference from the surroundings. It should therefore employ solutions to reduce background-noise interference and dynamic-range limitations.

The operation of the robot should not be slowed down by the sensor. Namely, a pose of the object should normally be estimated in 1 ms to 10 ms.

## 8.3   Technologies for Proximity Sensing

Proximity sensors have employed various transduction media, including sound waves, magnetic fields, electric fields, and light. Presently, electro-optical techniques seem to be the most appropriate for robotic-grasping applications. Such sensors are relatively small in size, have a large range of operation, and impose almost no restrictions on the object's material. However, recently, some new ultrasonic and capacitive proximity sensors have been fabricated directly as ICs, also showing the possibility of very-small-size proximity sensors based on these technologies [7, 8].

Brief descriptions of the principles of the primary technologies used by proximity sensors are given below, with the main emphasis being on optical transducers. A survey of commercial proximity sensors capable of measuring distances can be found in [6].
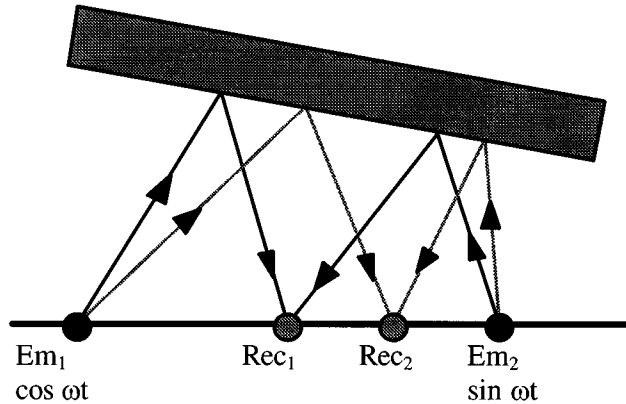
**FIGURE 8.2**    The basic phase-modulated proximity-sensor configuration.

## Electro-Optical Sensors

Many proximity sensors use light, directly scattered from a target surface, to determine the distance and orientation of the target object from the gripper. The mechanism by which light is reflected can be explained by a model that specifies four different reflection phenomena. According to this model, light reflects from the surface primarily as a result of one or more of the following interactions:

1. *Single surface reflection*: Light waves that reflect specularly a single time off a planar microfacet, whose dimensions are significantly larger than the wavelength.
2. *Multiple surface reflection*: Light waves that reflect specularly at least twice between multiple microfacets.
3. *Reflection after penetration*: Light waves that penetrate into the material, refract, and then reflect back out as diffused light.
4. *Corner reflection*: Light waves that diffract from interfaces with surface details about the same size or smaller than the wavelength (such as from corners of microfacets).

The primary phenomenon (1) usually exists in both dielectrics and metal. However, due to the high conductivity of metal surfaces, most of the light reflects specularly off the interface between the metal and the air, while the portion that penetrates into the metal surface is absorbed. Accordingly, the reflection intensity originating from internal refraction in metals is practically zero. In dielectrics, however, a large portion of the light penetrates into the surface, and then reflects back out as diffused light (3). The secondary phenomena (2) and (4) exist both in metals and dielectrics and add to the diffused reflectance.

Common measurement techniques used in optical proximity sensing utilize one or more of the reflected components to determine the pose of the object in relation to the transducer.

### Phase Modulation

A phase-modulated (PM) proximity sensor usually consists of two light sources and one or more photodetectors. The light sources are driven by modulated sinusoidal signals having a 90° phase relationship (Figure 8.2).

The emitter control voltages of the emitters, $V_{em1}$ and $V_{em2}$, have amplitudes of $a$ and $b$, respectively:

$$V_{eml}(t) = a \cdot \cos\omega t \tag{8.1}$$

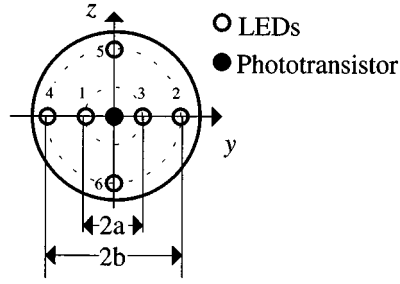$$V_{em2}(t) = b \cdot \sin\omega t \tag{8.2}$$

**FIGURE 8.3**  Sensor head reported in [9].

The signal detected by the receiver is a superposition of the two reflected signals, having corresponding attenuations of $A$ and $B$.

$$V_{rec}(t) = A \cdot V_{em1} + B \cdot V_{em2} \tag{8.3}$$

The signal attenuation is a function of the geometrical and electrical parameters of the sensor, the reflectivity characteristics of the object's surface, and the surface's distance and orientation with respect to the sensor. The combined signal at the receiver is therefore:

$$V_{rec}(t) = M \cdot \sin(\omega t + \phi) \tag{8.4}$$

where  $M$ = the combined attenuation-function, and
       $\phi$  = the combined phase-shift.

Usually, only the phase information $\phi$ is used, and the amplitude is completely neglected or used only for verifying the likelihood of error and its potential magnitude.

A proximity sensor that uses this technique has been reported in [9]. Figure 8.3 shows a *sensor head*; it comprises six light sources (LEDs) and a photodetector (a phototransistor). This sensor can measure the distance from the sensor's coordinate frame to the target point on the surface of the object ($x$), as well as the horizontal and vertical orientation of the object surface ($u$, $v$).

A simple model for the sensor was developed assuming that the light sources (LEDs) have low directivity, the photodetector (phototransistor) has high directivity, and the surface has diffused reflectivity. Figure 8.4 shows the basic configuration for the measurement of distance ($x$) and orientation ($u$ and $v$). Table 8.1 shows the combinations of the driving signals in each LED needed for the measurement of distance and orientation.

For the measurement of the distance $x$, LED1 and LED3 are modulated by $K_1 \sin\omega t$, and LED2 and LED4 by $K_2 \cos\omega t$, respectively. The brightness detected by the photodetector can be calculated (using Lambert's law) to be:

$$L_p = C \left( G_1 \frac{\cos(\alpha - v)}{a^2 + x^2} + G_2 \frac{\cos(\beta - v)}{b^2 + x^2} + G_3 \frac{\cos(\alpha + v)}{a^2 + x^2} + G_4 \frac{\cos(\beta + v)}{b^2 + x^2} \right) \tag{8.5}$$

where $G_i$ ($i$ = 1, 2, 3, 4) are the intensities of the light sources, and $C$ is the reflection factor of the surface at point $P$. Considering that for this case: $G_1 = G_3 = K_1 \sin\omega t$, $G_2 = G_4 = K_2 \cos\omega t$, $\cos\alpha = x/\sqrt{a^2 + x^2}$ and $\cos\beta = x/\sqrt{b^2 + x^2}$, Equation 8.5 can be rewritten as:
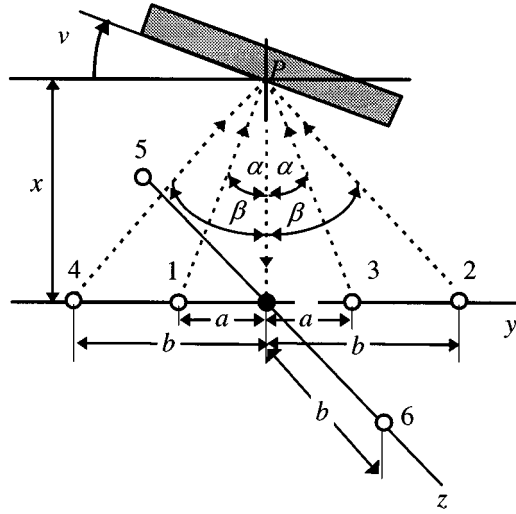
**FIGURE 8.4**  Measurement parameters for the sensor reported in [9].

**TABLE 8.1**  Combinations of the LED Driving Signals

| Mode | LED1 | LED2 | LED3 | LED4 | LED5 | LED6 |
|---|---|---|---|---|---|---|
| Distance $(x)$ | $\sin \omega t$ | $\cos \omega t$ | $\sin \omega t$ | $\cos \omega t$ | — | — |
| Orientation $(u)$ | — | $\cos \omega t$ | — | $\sin \omega t$ | — | — |
| Orientation $(v)$ | — | — | — | — | $\cos \omega t$ | $\sin \omega t$ |

$$L_{\mathrm{p}} = 2Cx \left\{ \frac{K_1}{\left(a^2 + x^2\right)^{3/2}} \sin \omega t + \frac{K_2}{\left(b^2 + x^2\right)^{3/2}} \cos \omega t \right\} \cos v = M \sin\left(\omega t + \phi_{\mathrm{x}}\right) \qquad (8.6)$$

The amplitude $M$ and the phase shift $\phi_{\mathrm{x}}$ are given by:

$$M = 2Cx \left\{ \frac{K_1^2}{\left(a^2 + x^2\right)^3} + \frac{K_2^2}{\left(b^2 + x^2\right)^3} \right\}^{1/2} \cos v \qquad (8.7)$$

and

$$\phi_{\mathrm{x}} = \tan^{-1} \left[ \frac{K_2 \left(a^2 + x^2\right)^{3/2}}{K_1 \left(b^2 + x^2\right)^{3/2}} \right] \qquad (8.8)$$

From Equation 8.8, it can be observed that the distance $(x)$ can be obtained from $\phi_{\mathrm{x}}$. It is important to note that, in theory, the calculation is not affected by the reflection factor $(C)$ of the surface.
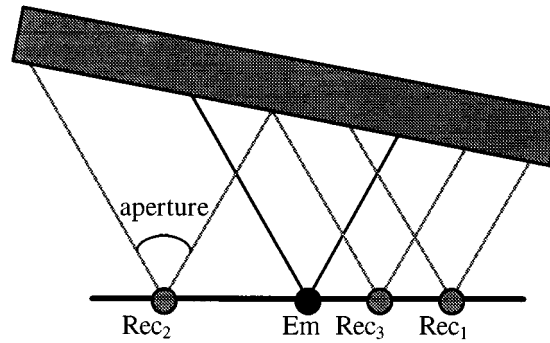
**FIGURE 8.5** The basic amplitude-modulated proximity sensor configuration.

Similarly, the orientation angles $u$ and $v$ can be obtained by driving the LEDs as indicated in Table 8.1. For example, $v$ can be determined by modulating LED4 and LED2 by the signals $K_1\sin\omega t$ and $K_2\cos\omega t$, respectively. For this case, the phase shift associated with the brightness of the object at point $P$ is given by:

$$\phi_v = \tan^{-1}\left[\frac{K_2\left(x - b\tan v\right)}{K_1\left(x + b\tan v\right)}\right] \tag{8.9}$$

Note that, in order to recover $v$ from Equation 8.9, $x$ must be known. Accordingly, the distance $x$ must be determined first. Correspondingly, the orientation angle ($v$) can be calculated from the new phase shift $\phi_v$. The angle $u$ can be calculated by modulating LED6 and LED5 with $K_1\sin\omega t$ and $K_2\cos\omega t$, respectively, and then determining the corresponding phase shift of the associate brightness at point $P$.

The pose-estimation results using this sensor were quite satisfactory and showed a good agreement between the theory and experiment.

In [10], an experimental setup of a PM distance sensor, similar to the one in [9], was reported for investigating the effect of the geometric and electronic parameters on the performance of the sensor. Optimal parameters were obtained for some targeted sensor-operation characteristics.

### Amplitude Modulation

In amplitude-modulated (AM) sensors, the magnitude of the light reflected from a surface is utilized to determine the pose of the object.

AM transducers usually consist of one light source and several photodetectors (Figure 8.5). They were redesigned and optimized several times over the past decade to yield better measurement accuracy [11–14].

Many AM proximity sensors utilize optical fibers to illuminate and collect light from the surfaces of objects. The use of optical fibers, in a Y-guide configuration (Figure 8.6), facilitates the operation of sensitive low-noise circuitry in a shielded environment appropriately remote from the robot's electro-magnetic interference sources.

AM transducers primarily use variations of the basic Y-guide transducer. Two important parameters can be varied in the design of Y-guides: the distance, $d$, between the emitting and receiving fibers (referred to hereafter as the emitter and the receiver, respectively), and the inclination angle, $\vartheta$, of the receiver fiber with respect to the transducer's surface. The emitter is usually placed perpendicular to the transducer's surface, due to symmetry requirements, as will be explained later in this section.

The collection of a sufficient amount of reflected light requires the use of relatively wide-diameter fibers, typically having a 0.3 mm to 2 mm core size. This requirement demands the use of relatively low-grade plastic fibers. Although attenuations of up to 1 dB m$^{-1}$ are common in such plastic fibers, this loss rate is relatively insignificant for Y-guide applications because of the short length of the cables normally used. The numerical aperture (NA) of the plastic fibers, on the other hand, is an important parameter
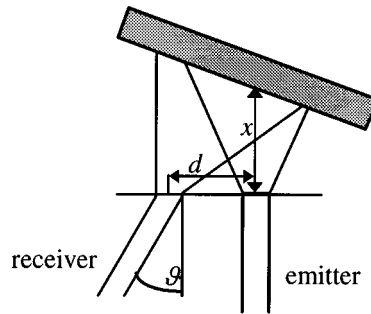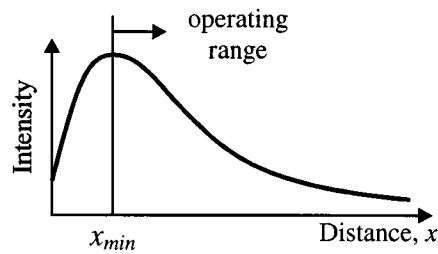
**FIGURE 8.6**    Y-guide transducer.



**FIGURE 8.7**    Y-guide response for distance measurement.
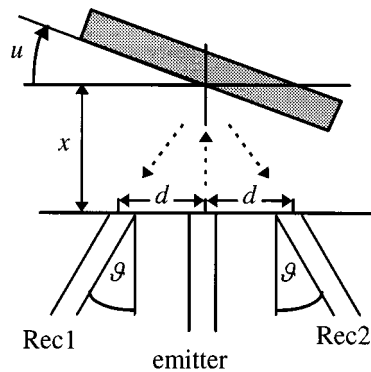


**FIGURE 8.8**    Typical receiver-pair constellation for orientation measurements.

in the transducer design, since lenses are rarely used in conjunction with AM-type transducers. In particular, the acceptance angle of the fiber is fixed and given by $\alpha = 2\sin^{-1} NA$.

For a Y-guide, the intensity of the light reflected from the surface is not a monotonic function of the distance. Thus, the minimum operating distance of the transducer ($x_{min}$) is usually limited to a value that will guarantee a monotonic response (Figure 8.7).

For the measurement of surface orientation, a symmetrical three-fiber constellation (Figure 8.8) can be used. In this Y-guide configuration, the emitter is at the center and the two receivers are positioned symmetrically on either side [12]. The light intensities detected by the receivers, for the transducer shown in Figure 8.8, are illustrated in Figure 8.9 as a function of the surface orientation.

In the usual operating range of an AM transducer, the intensity of the light at the receiver is inversely related to the distance squared. As a result, it is conceptually possible to configure a transducer such that
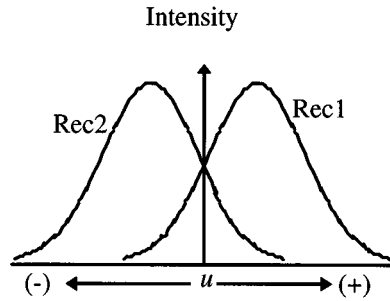
**FIGURE 8.9**  The light intensity detected by each receiver as a function of the surface orientation ($u$).
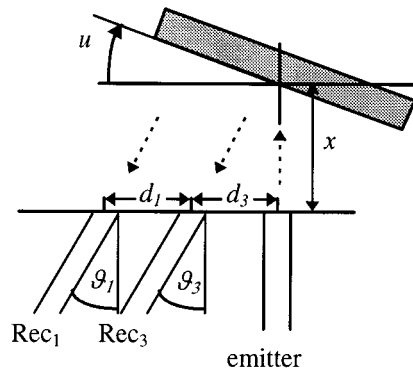


**FIGURE 8.10**  An asymmetrical receiver-pair constellation for distance measurements.

its sensitivity and accuracy will increase as the gripper nears the contact point, at which both the distance and the orientation of the object's surface are zero [10, 12]. However, in practice, because of the limited dynamic range of the electronic transducer interface, a trade-off exists between the desired maximum accuracy near contact, and the maximum range of operation. These and other considerations must be taken into account when establishing the geometric features of the transducer.

Another important factor to take into account in the design of an AM sensor is the need to reduce, as much as possible, the effect of the variation in the emitting power of the light source, $P_o$, on the transducer's measurements. This normally leads to the employment of a pair of receivers. A normalized differential voltage (DV) estimation scheme, such as the following, is then applied to the pair of measurements:

$$DV = \frac{V_{rec_1} - V_{rec_2}}{V_{rec_1} + V_{rec_2}}  \tag{8.10}$$

where $V_{rec_1}$, $V_{rec_2}$ are the voltages measured by receivers 1 and 2. However, in order to eliminate the effect of $P_o$ on DV, each receiver must linearly convert the light intensity to a corresponding voltage measurement.

In order to use a DV scheme for the measurement of distance, an asymmetrical transducer configuration can be used (Figure 8.10). However, one must note that, although orientation measurements are not affected by variations in distance, distance measurements are significantly affected by the orientation of the surface, e.g., [15].

Accordingly, in using an AM proximity sensor with a DV scheme, the orientation is first approximated, and subsequently the distance is determined. The accuracies of the measured distance and orientation angle can be further improved by an iterative process.
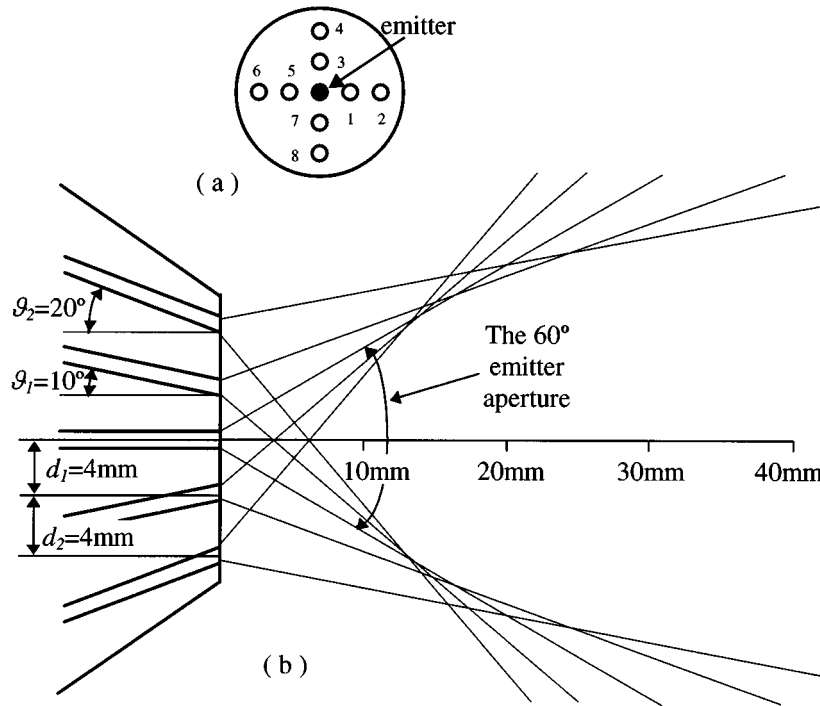
**FIGURE 8.11**  AM transducer design for the sensor reported in [14]: (*a*) top view; (*b*) front view.

Based on the above issues and observations, the outputs of the three receivers of the basic AM proximity sensor (Figure 8.5) can be paired for measuring both distance and orientation: the pair $rec_1$-$rec_2$ can be used for orientation measurement, while the pair $rec_1$-$rec_3$ can be used for distance measurement.

An experimental AM proximity sensor, capable of estimating the pose of an object with high accuracy, was reported in [14, 16, 17]. The transducer consists of one emitter, placed perpendicularly to the sensor head, and eight inclined receiver elements (Figure 8.11). The receivers of this transducer were paired for the specific measurements of distance, as well as of the vertical or horizontal orientation. However, the pose of the surface was determined with higher accuracy by using a polynomial fit technique (as opposed to the DV scheme described above), that provided relationships between the individual estimated parameters (*x*, *u*, and *v*) and all eight signals received.

The sensor presented in [14], and shown in Figure 8.11, operates in the range of 0 mm to 50 mm and ±20°. It can achieve an accuracy of 6.25 μm in distance and an accuracy of 0.02° in angular measurements in the near-contact region (0 mm to 6 mm range), using a general calibration-per-group strategy for different material groupings. This implies that the measured object's material belongs to a calibration group, which includes similar object surface characteristics; for example, machined metals. Better accuracies can be achieved using a calibration-per-surface strategy.

A similar configuration to the one shown in Figure 8.11 was reported earlier in [18] for the measurement of distances, where the orientations of each receiver pair relative to the emitter $\vartheta_1$ and $\vartheta_3$ were set at 10°. However, in this case, the apertures of the emitter and receiver were severely restricted by a collimating graded index (GRIN) lens. The emitter diameter was larger than that of the receivers in order to transmit more light. The measurements of the transducer were then processed in two phases: (1) the DVs of all the receiver pairs were processed independently to provide four distance estimations; and, (2) the four distance estimations were then averaged to provide a more accurate estimate, eliminating adverse effects due to variations in surface orientation.
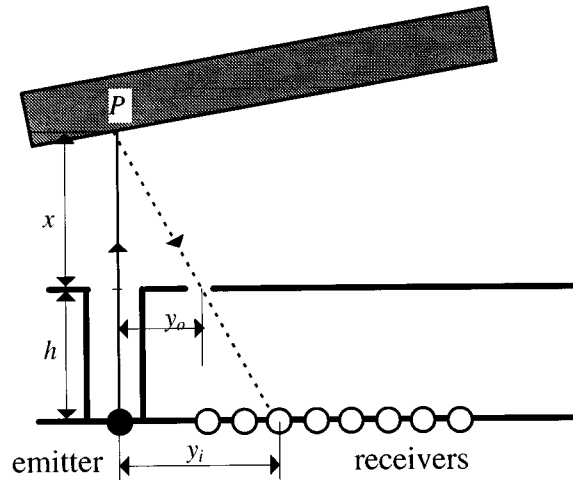
**FIGURE 8.12**    Basic principle of a proximity sensor for measuring distance based on triangulation.

## Geometrical Techniques

Proximity sensors based on geometrical techniques determine the pose of the object by examining the geometrical attributes of the reflected and incident light beams. Two of these techniques, one based on triangulation and the other based on the Gaussian lens law, are presented here.

Figure 8.12 shows the basic configuration of a proximity transducer for measuring distance ($x$) based on the triangulation technique [19, 20]. The sensor head consists of a laser light source and a linear array of photodetectors ($R_i$, with i = 1, 2, …, $n$). A narrow light beam illuminates point $P$, and the receivers detect the reflected light from the illuminated point through a transmitting slit. The geometry of the ray trajectory provides the basic information for the estimation of the distance ($x$). While the light source illuminates the surface of the object, the photodetector array is scanned to detect the light path used for making the output signal maximum. The light path obtained by this scanning is called the effective light path [19]. This light path is the one indicated in Figure 8.12. The distance ($x$) can be determined by accurately detecting the position ($y_i$) and precisely measuring the dimensions ($h$) and ($y_o$),

$$\frac{x}{x+h} = \frac{y_o}{y_i} \tag{8.11}$$

or

$$x = \frac{y_o h}{y_i - y_o} \tag{8.12}$$

In [26], it is claimed that such a sensor has the following properties: (1) the influence of irregularities, reflectivity, and orientation of the object is negligible; (2) the distance measurement is not affected by illumination from the environment and luminance of the object (their influence is eliminated by comparison of two sensor signals obtained in successive on-and-off states of the light source); and (3) the sensor head is sufficiently small to be used in a robot hand.

An experimental proximity sensor configuration, based on triangulation and capable of measuring both distance and orientation, is shown in Figure 8.13 [21]. The sensor uses six infrared LEDs as light sources, an objective lens, and an area-array detector chip for detecting spot positions. The directions of
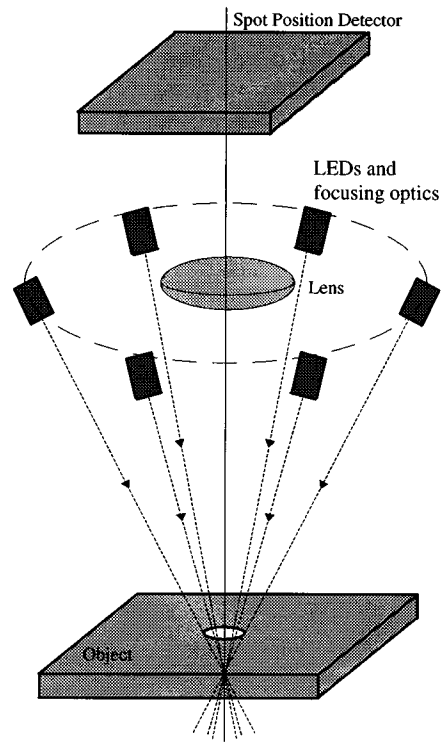
**FIGURE 8.13**  Multilight source proximity sensor reported in [21].

the beams are aligned to form a fixed cone of light. This sensor is of a type called scanning-emitter since each LED is sequentially pulsed to perform the measurements. As each LED is sequentially pulsed, the sensor IC detects the position of the spot projected by the reflected light beam from the object's surface. Knowledge of the spot's position, together with the camera's optics and the trajectory of each light beam, can be used to perform a triangulation to determine the three-dimensional coordinates of each light spot on the target surface. A set of six 3-D points are obtained for the six LEDs. Then, by fitting a plane to those points, the distance and orientation of the object's surface are approximated.

Another scanning-emitter-type proximity sensor was reported in [22]. In this case, a mechanical scanning system was utilized. One notes that inherent problems with sensors that use mechanical scanning devices include lower reliability and increased overall size.

Some recently reported triangulation sensors are sufficiently small in size to be mounted on a gripper [5]. However, they are still susceptible to errors due to distortion and separation of the light beam's reflection caused by surface irregularity, and can also have blind spots as a result of discontinuities associated with the shape of the sensed object.

Another group of geometrical electro-optical proximity sensors are those based on the Gaussian lens law [23, 24]. The basic configuration of such a transducer is shown in Figure 8.14. A light beam, collinear to the optical axis, forms a spot on the target's surface. The light scattered from the spot is collected by the lens. In Figure 8.14, PN represents the limiting ray that can be collected by the lens. The target distance ($x$) can be calculated in terms of the focal length of the lens ($f$) and the image position ($w$). Applying the Gaussian lens law, the distance $x$ can be calculated as:
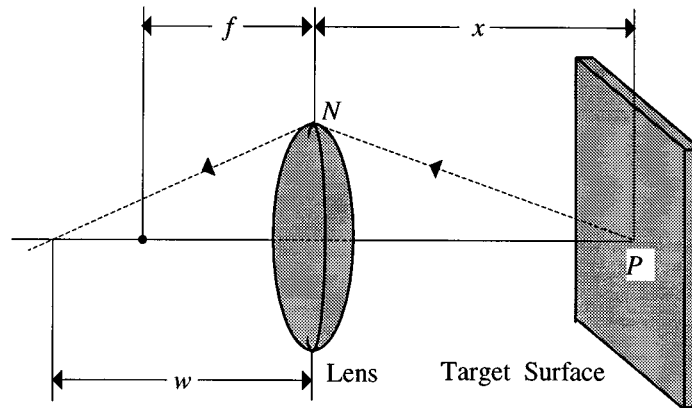
$$x = \frac{fw}{w - f} \tag{8.13}$$

**FIGURE 8.14**    The principle of proximity sensing based on the Gaussian lens law reported in [7].
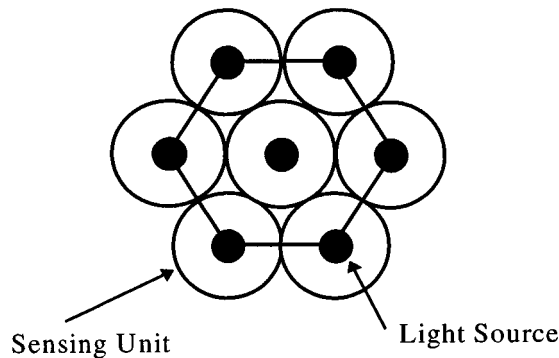


**FIGURE 8.15**    Configuration of HexEye (top view).

A proximity sensor (the HexEye) based on this lens principle is shown in Figure 8.15 [23, 24]. The sensor consists of seven identical "sensing units" arranged in a hexagonal pattern. Each sensing unit in turn comprises four main parts: an objective lens, a conical mirror, six linear receiver arrays, and a laser diode light source.

The light beam generated by a light source forms a spot on the target surface, and the light flux scattered from the spot is collected by the objective lens and projected onto the receiver arrays in each sensing unit. The target distance is determined by the position, size, and shape of an image formed on individual receiver arrays of the unit.

The sensor operates in two modes, either distance or orientation. In the distance measurement mode, the seven light sources are activated one at a time to generate a light spot on the target surface, while all the sensing units receive the light flux scattered from the same light spot. The active unit determines the distance using the principle of the Gaussian lens law, while the nonactive units determine the distance based on triangulation. For the orientation measurement mode, the seven sensing units are grouped into orientation measurement units (OMUs). Each OMU comprises three neighboring sensing units around the center, resulting in a total of six possible OMUs. The local orientation of the surface is estimated by integrating the six orientation measurements.

The mapping between the light distribution on the arrays of light detectors and the target distance is obtained through calibration. Using the light distribution (instead of light intensity as in the case of AM sensors), it is intended that the mapping be independent of surface properties such as color, material, diffusion, and reflectance factors. However, it has been shown that the mapping may be corrupted by "noise" from several sources, including reflection patterns and ambient light.
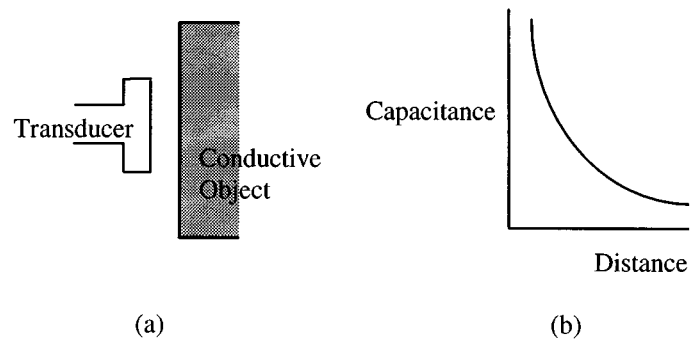
**FIGURE 8.16** Capacitive proximity sensor based on the principle of parallel plates, (*a*) structure and (*b*) sensor response.

Using the Gaussian lens law has the following advantages over the triangulation principle: (1) the light source can be located at the center of the objective lens, allowing not only the sensor to be compact, but also the amount of light flux input to the lens to be maximized, and (2) the sensitivity can be optimized for a certain range of measurement distance by controlling *f*.

### Time-of-Flight

Time-of-flight-measuring electro-optical sensors are radar-type systems. However, unlike regular radar, which transmit a pulse of radio-frequency energy, these sensors normally use a modulated light beam. The distance to the target is extracted from the measured phase shift of the reflected light. Two problems associated with such sensors are: difficulty in measuring short distances (which requires a very high modulation frequency), and the need for a mechanical scanning/switching system to get additional information (such as orientation) [5, 25].

### Photothermal Effect

The photothermal effect transducer uses a strong light beam directed toward the object's surface. The distance to the object is extracted from measurements of the thermal wave generated by the light absorbed by the object. The detection scheme and signal processing are similar to those used in an AM sensor. Since the shape of the thermal wave generated at the surface is surface-texture independent, the photothermal sensor does not suffer from the surface robustness problem associated with AM sensors. However, the photothermal sensor is rather slow, and limited to highly absorbing surfaces [26].

## Capacitive Sensors

Capacitive sensors generate and measure changes in an electric field caused by either a dielectric or conducting object in their proximity.

There are basically two types of capacitive proximity sensor. One type uses the principle of a parallel plate capacitor, the other uses the principle of fringing capacitances [8, 27, 28]. For the parallel plate type proximity sensor, the transducer forms one plate and the object measured forms the other plate. The structure of a parallel plate type proximity sensor and its typical response are shown in Figure 8.16 [8].

The parallel plate type proximity sensor is widely applied in industry. However, this type of a sensor has three major limitations: (1) the object being measured must be conductive; (2) the inverse gap-capacitance relationship is highly nonlinear and (3) the sensitivity drops significantly in the case of large gaps.

The second type of capacitive proximity sensor uses the principle of fringing capacitance [8]. The sensor has two "live" electrodes and the object being measured does not need to be part of the sensor system. The target object could be either conductive or nonconductive. However, the measurement of distances is affected by the type of object material. Therefore, separate calibrations must be carried out for different materials.
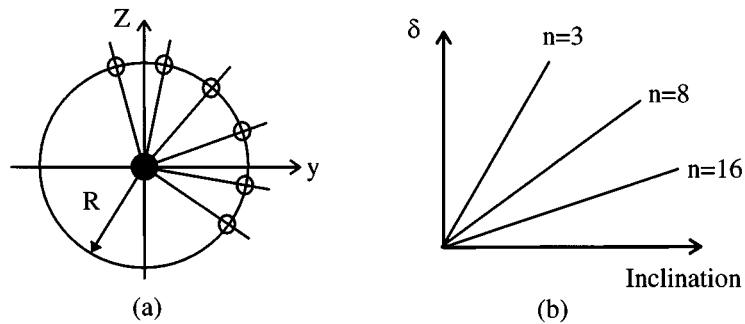
**FIGURE 8.17**   (*a*) Configuration of the ultrasonic sensor and (*b*) surface inclination versus δ.

In [30], an innovative capacitive microsensor was presented. Using micromachining technology, the electrode thickness can be significantly reduced and the fringing effect increased when compared with other capacitive sensors. Consequently, this sensor yields a better sensitivity. An array of such transducers can be implemented to measure the distance and orientation of an object.

Proximity capacitive sensors have the following general advantages: (1) low energy consumption and (2) simple structure. The major disadvantages, however, are that they are influenced by external signals and a calibration-per-surface technique must be carried out, since their operation directly depends on the object's material.

## Ultrasonic Sensors

The basic principle underlying ultrasonic ranging sensors is the measurement of the time required for a sound wave to travel from the emitter to the object's surface and return to the detector. By using several such emitters and detectors, one can obtain information about the distance and orientation of the surface.

In [19], a novel method is proposed to measure the orientation angles of an object's surface using the phase differences of reflected echoes. Figure 8.17(*a*) shows the configuration of a planar sensor head with *n* receivers, which are equally spaced and located on a circle of radius *R* around the transmitter T. A linear relationship exists between the difference in lengths, δ, of two reflecting paths for an adjacent pair of receivers and the object inclinations.

In Figure 8.17 (*b*), the relationship between the inclination of the target surface and δ is shown. It can be observed that the measuring range of the sensor can be enlarged with an increase in the number of receivers. In [29], it is also shown that the measuring range can be enlarged by reducing *R*. However, it was noted that measurements carried out with a small sensor are potentially less accurate.

Experimental results using a transducer with six (*R* = 30 mm) and eight (*R* = 20 mm) receivers were reported in [29]. With the six-receiver transducer, the measuring range of the orientation angles was ±15°; while for the eight-receiver transducer, the maximum measuring range was ±30°. With the six-receiver transducer, the orientation angle could be determined with an accuracy of 0.5°, in the measuring range of ±15°, and 0.2° when the range was restricted to ±5°.

One of the major disadvantages of ultrasonic proximity sensors is that they are relatively large in size. However, implementing these sensors using micromachining could solve this problem. In [7], the generation and detection of ultrasound, for proximity sensing, was investigated using micromachined resonant membrane structures.

## Magnetic Sensors

A magnetic-type sensor creates an alternating magnetic field, whose variation provides information about the object's position.

The simplest magnetic sensors are reed microswitches or Hall effect switches. However, the most commonly used sensors in robotics are based on the electromagnetic inductive principle, emphasizing

eddy current generation. The basic principle consists of creating a magnetic field using appropriate coils around a core with high permeability and an oscillator with a frequency excitation high enough to minimize the penetration of the field inside a conductive material. The main problems with magnetic sensors are their high size/range ratio and difficulty in providing reliable distance measurements in varying magnetic environments.

## Acknowledgments

## References

1. H. R. Everett, *Sensors for Mobile Robots: Theory and Application,* Natick, MA: A. K. Peters, Ltd., 1995.
2. B. Espiau, An overview of local environment sensing in robotics applications, *Sensors and Sensory Systems for Advanced Robots, NATO ASI Series,* F43, 125-151, 1988.
3. W. D. Koenigsberg, Noncontact distance sensor technology, *SPIE, Intelligent Robots,* 449, 519-531, 1988.
4. Å. Wernersson, B. Boberg, B. Nilsson, J. Nygårds, and T. Rydberg, On sensor feedback for gripping an object within prescribed posture tolerances, *IEEE, Int. Conf. on Robotics and Automation,* Nice, France, 1992, 1654-1660.
5. A. Bradshaw, Sensors for mobile robots, *Measurement and Control,* 23(2), 48-52, 1990.
6. R. Volpe and R. Ivlev, A survey and experimental evaluation of proximity sensors for space robotics, *IEEE Int. Conf. on Robotics and Automation,* 4, 3466-3473, 1994.
7. O. Brand, H. Baltes, and U. Baldenweg, Ultrasound-transducer using membrane resonators realized with bipolar IC technology, *IEEE Conf. on Micro Electro Mechanical Systems,* Oiso, Japan, 1994, 33-38.
8. R. C. Luo and Z. Chen, Modeling and implementation of an innovative micro proximity sensor using micromachining technology, Proc. *IEEE/RSJ Int. Conf. Intelligent Robots and Systems,* Yokohama, Japan, 1993, 1709-1716.
9. R. Masuda, Multifunctional optical proximity sensor using phase modulation, *J. Robotic Systems,* 3(2), 137-147, 1986.
10. O. Partaatmadja, B. Benhabib, and A.A. Goldenberg, Analysis and design of a robotic distance sensor, *J. Robotic Systems,* 10, 427-445, 1993.
11. O. Partaatmadja, B. Benhabib, A. Sun, and A. A. Goldenberg, An electrooptical orientation sensor for robotics, *IEEE Trans. on Robotics and Automation,* 8, 111-119, 1992.
12. O. Partaatmadja, B. Benhabib, E. Kaizerman, and M.Q. Dai, A two-dimensional orientation sensor, *J. Robotic Systems,* 9, 365-383, 1992.
13. P. P. L. Regtien, Accurate optical proximity detector, *IEEE Conf. on Instrumentation and Measurement Technology,* San Jose, CA, 1990, 141-143.
14. A. Bonen, R. E. Saad, K. C. Smith, and B. Benhabib, Active-sensing via a novel robotic proximity sensor, *Int. Conf. on Recent Advances in Mechatronics (ICRAM'95),* Istanbul, 1995, 1053-1058.
15. Y. F. Li, Characteristics and signal processing of a proximity sensor, *Robotica,* 12, 335-341, 1994.
16. A. Bonen, R. E. Saad, K. C. Smith, and B. Benhabib, A novel calibration technique for electro-optical proximity sensors, *Int. Conf. on Industrial Electronics, Control and Instrumentation (IECON'95),* Orlando, FL, 1995, 1190-1195.
17. A. Bonen, R. E. Saad, K. C. Smith, and B. Benhabib, A novel optoelectronic interface-circuit design for sensing applications, *IEEE Trans. Instrum. Meas.,* 45, 580-584, 1996.
18. H. Bukow, Fiber optic distance sensor for robotic applications, *SME Conf., Sensors,* MS86-938, Detroit, MI, 1986.
19. T. Okada, Development of an Optical Distance Sensor for Robots, *Int. J. Robotics Res.,* 1, 3-14, 1982.

20. M. A. Kujoory, Real-Time Range and Elevation Finder, *Proc. IEEE,* 72(12), 1821-1822, 1984.
21. M. Fuhrman and T. Kanade, Optical proximity sensor using multiple cones of light for measuring surface shape, *Optical Eng.,* 23, 546-553, 1984.
22. T. Okada and U. Rembold, Proximity sensor using a spiral-shaped light-emitting mechanism, *IEEE Trans. on Robotics and Automation,* 7, 798-805, 1991.
23. S. Lee, Distributed optical proximity sensor system: HexEYE, *IEEE Int. Conf. Robotics and Automation,* 2, 1567-1572, Nice, France, 1992.
24. S. Lee and J. Desai, Implementation and evaluation of HexEye: a distributed optical proximity sensor system, *Proc. IEEE Int. Conf. Robotics and Automation,* 3, 2353-2360, Nagoya, Aichi, Japan, 1995.
25. S. Shinohara et al., Compact and high precision range finder with wide dynamic range using one sensor head, *IEEE Conf. Instrumentation and Measurement Technology,* Atlanta, GA, 1991, 126-130.
26. M. Ito, K. Hane, F. Matsuda, and T. Goto, Proximity sensing technique using the photothermal effect, *J. Japan Soc. Precision Eng.,* 58, 139-144, 1992.
27. B. E. Noltingk, A novel proximity gauge, *J. Scientific Instruments, Series 2,* 2, 356-360, 1969.
28. B. E. Noltingk, A. E. T. Nye, and H. J. Turner, Theory and application of a proximity gauge using fringing capacitance, *Proc. ACTA IMEKO,* 1976, 537-549.
29. S. Nakajima and Y. Takahashi, An ultrasonic orientation sensor with distributed receivers, *Advanced Robotics,* 4, 151-168, 1990.
30. A. Moldoveanu, Inductive proximity sensors, fundamentals and standards, *Sensors,* 10(6), 11-14, 1993.